IEEE Access
Multidisciplinary ⋮ Rapid Review ⋮ Open Access Journal

Received 25 May 2022, accepted 13 June 2022, date of publication 21 June 2022, date of current version 27 June 2022.

Digital Object Identifier 10.1109/ACCESS.2022.3185136

Hybrid Precoding for Millimeter Wave MIMO: Trace Optimization Approach

PRABHAT RAJ GAUTAM, (Graduate Student Member, IEEE), AND LI ZHANG, (Senior Member, IEEE)
School of Electronic and Electrical Engineering, Institute of Communication and Power Networks, University of Leeds, Leeds LS2 9JT, U.K.
Corresponding author: Li Zhang (l.x.zhang@leeds.ac.uk)

ABSTRACT The hybrid precoding problem in point-to-point millimeter wave (mmWave) multiple input multiple output (MIMO) for narrowband channel has been established as a Frobenius norm minimization problem. It is translated into trace minimization problem, and two algorithms are proposed to solve it. In the first method based on alternating minimization, we alternately determine the analog precoder and digital precoder, keeping the other constant to minimize the trace. The analog precoding subproblem with the fixed digital precoder is converted into a semi-definite programming (SDP) problem and solved by block coordinate descent (BCD) algorithm with suitable modifications. In the second method, we segregate the analog precoding and digital precoding subproblems by considering orthogonality of analog precoder. The analog precoding is further rephrased as a trace maximization problem and solved by an iterative power method by enforcing orthogonality constraint on the analog precoder. The adapted form of modified Gramm-Schmidt orthogonalization procedure is employed to impose orthogonality on the analog precoder. The proposed methods are extended for wideband channel by considering orthogonal frequency division multiplexing (OFDM). The proposed methods not only exhibit a good performance but also come with lower computational complexity when compared to existing methods with comparable performances.

INDEX TERMS Millimeter wave (mmWave) communication, hybrid precoding, trace optimization, alternating minimization, block coordinate descent, power method.

I. INTRODUCTION

Millimeter wave (mmWave) tenders a huge unused bandwidth for wireless communication which have made mmWave communication an attractive prospect for the researchers [1]–[3]. However, mmWave signals undergo huge attenuation due to severe propagation and penetration losses as their smaller wavelengths make them susceptible to absorption or scattering by gases and rain [4], [5]. In order to compensate for the high attenuation, large antenna arrays need to be employed. The radio frequency (RF) chains that operate at mmWave frequency are costly and consume high power. Thus, employing fully digital precoding in mmWave multiple-input multiple-output (MIMO) is an impossible prospect, owing to power consumption and cost concerns [6], [7]. Hybrid precoding is the technique that has surfaced as the most promising solution to address the precoding problem in mmWave MIMO. In hybrid precoding, the transmit signals undergo fully digital precoding at much lower dimension compared to the number of transmit antennas, and the digitally precoded signals are fed through analog precoder or beamformer before transmitting [8]. The hybrid precoding requires architecture different from conventional MIMO architecture called hybrid architecture in which the number of RF chains is very small compared to the number of antennas, and usually a network of phase shifters is used to execute analog precoder. Sometimes the inverters and switches are also used in place of phase shifters to encourage energy efficiency [9], [10]. The hybrid architectures are "fully connected" if each RF chain is connected to all of the antennas and "partially connected" if each RF chain is connected to only a subset of the antennas.

The hybrid precoder is computed as the product of analog precoder and digital precoder and the computation of hybrid precoder poses a problem because each element of analog precoding matrix needs to satisfy unit modulus constraint which is non-convex. The hybrid precoding for point-to-point MIMO is considered in [11] and it is proposed that

The associate editor coordinating the review of this manuscript and approving it for publication was Adao Silva.

hybrid precoder can be determined by minimizing Euclidean distance between optimal fully digital precoder and hybrid precoder. The authors treat hybrid precoding as a sparse reconstruction problem to formulate orthogonal matching pursuit (OMP) based precoding algorithm. Both [12] and [13] propose hybrid minimum mean square error (MMSE) precoders based on OMP. The OMP-based precoders, though low on complexity, require a large number of RF chains to offer good performance.

The works in [14]–[16] present the hybrid precoders for multiple user MIMO where the analog precoders are built from codebooks, similar to [11]–[13]. The precoders based on codebook are limited in performance as there is restriction to choose columns of analog precoder from the codebook. The authors of [17] propose hybrid precoders based on heuristic design to maximize spectral efficiency for point-to-point MIMO and multi-user multiple-input single-output (MU-MISO) systems. It is also established that the minimum number of RF chains required to achieve the performance of a fully digital precoder is double the number of transmit data streams [17].

[18] proposes several strategies to design hybrid precoders, *viz.*, HD-AM, HD-FUM, HD-CVXR and HD-LSR. HD-AM is based on alternating minimization for the case where RF chains are in equal number to data streams and in HD-FUM the columns of analog precoder are chosen from dictionary based on correlations. The analog precoder is computed using iterative methods by optimizing per each of its column at a time with fixed digital precoder in HD-CVXR, and in HD-LSR each entry of analog precoder is updated using least squares solution. The HD-LSR precoder is very good in performance and not high on complexity but it is only designed to work in narrowband channel. The authors in [19] show how the performance of optimal fully digital precoder can be attained when the number of RF chains is twice the number of transmit data streams. It is also shown that if two phase shifters and an adder are available per each RF chain, the performance of optimal precoder is achievable even when the RF chains are equal in number to transmit symbols.

Several hybrid precoding methods based on alternating minimization are presented in [20]. The authors propose an algorithm based on manifold optimization (MO) called MO-AltMin and PE-AltMin algorithm by imposing orthogonality on digital precoder for the fully-connected architecture and an algorithm based on semi-definite relaxation (SDR) for partially-connected architecture. The PE-AltMin algorithm, despite its low complexity, is disadvantaged as its performance does not grow even if the number of RF chains is increased beyond the number of transmit data streams. [21] proposes MO-based hybrid precoder to minimize mean square error. The MO-based algorithms offer better performance, albeit at the cost of higher complexity. The hybrid MMSE precoder in [22] uses generalized eigenvector decomposition (GEVD) in iterative manner. [23] considers fully connected and partially-connected architectures, and proposes separate algorithms based on majorization-minorization and minorization-majorization respectively. The proposed algorithms are very low on complexity.

In [24], authors decouple the hybrid precoding problem into quadratically constrained quadratic programming (QCQP) sub-problem and least-squares sub-problem with unit-modulus constraint. The new sub-problems are solved by alternating optimization technique and three different algorithms, namely, SDR-AO, ADMM-AO and ACMF-AO. Among the proposed algorithms, SDR-AO, an SDR-based algorithm that is solved by convex optimization toolbox CVX [25], offers very good performance but suffers from high computational complexity. The vectorization of the original problem which is in matrix form converts it into a high dimensional problem and hence the complexity of the proposed methods is extremely high. MO-AltMin algorithm in [20] suffers from the same problem.

We start with the optimal fully digital precoder and proceed to determine the hybrid precoder by minimizing the Frobenius norm of the difference of optimal precoder and the hybrid precoder as proposed in [11]. We translate the Frobenius norm minimization problem into trace optimization problem by replacing the Frobenius norm with equivalent trace form. The contributions we have made are:

(i) We develop an algorithm based on alternating minimization where we try to optimize the objective function keeping one of the digital precoder or analog precoder constant at a time. The optimal digital precoder that minimizes the objective function with the fixed analog precoder is computed using Lagrangian method. As for the analog precoder determination problem with the fixed digital precoder, we translate the problem into semi-definite programming (SDP) problem by convex relaxation. The subproblem is similar to the standard SDP found in PhaseCut problem [26], but with some additional constraints. The subproblem can be solved by CVX [25]. However, we use modified form of Block Coordinate Descent (BCD) algorithm [27] to solve the analog precoding subproblem and hence we refer the hybrid precoding algorithm by the name MBCD-HP. The SDR-AO algorithm in [24] also converts the hybrid precoding problem into SDP problem and solves it by using CVX. However, there are significant differences in its approach and our approach in MBCD-HP. SDR-AO converts the hybrid precoding problem into vector form and finally forms an SDP problem which adds a high complexity. However, in MBCD-HP we operate in matrix form without converting into vector form to convert precoding problem into an SDP problem which helps in restricting the complexity. To the best of our knowledge, there has not been any prior work that utilizes such SDP based algorithms on hybrid precoding or similar problem directly in matrix form without converting the problem into vector form.

(ii) In another hybrid precoding algorithm, we decouple the hybrid precoding problem into analog precoding and digital precoding subproblems by substituting the least squares solution for digital precoder with fixed analog precoder into the trace form of the original objective function. We further simplify the expression by making suitable assumptions about the orthogonality of the analog precoder, and then form the new analog precoding subproblem by imposing the orthogonality constraint on analog precoder. We develop a simple algorithm called Iterative Power Method- Hybrid Precoding (IPM-HP) based on iterative power method to solve for the optimal analog precoder. With the analog precoder computed, the digital precoder is determined by the least squares solution of the original objective function.

(iii) The two hybrid precoding algorithms are developed by considering narrowband channel model. We further extend the algorithms for wideband channel by considering orthogonal frequency division multiplexing (OFDM).

(iv) We compute the computational complexities of the proposed hybrid precoding algorithms and compare with the existing algorithms. We demonstrate through simulations that the proposed method MBCD-HP not only performs close to high performance precoders like MO-AltMin, HD-LSR and SDR-AO but also involves smaller complexity compared to the MO-AltMin and SDR-AO algorithms. The IPM-HP displays slightly lower performance but it entails significantly low complexity.

A. ORGANIZATION OF THE PAPER

The rest of the paper is organized as follows. In section II, we define the system modeling, channel model, and introduce the hybrid precoding problem. The section III formulates the analog and digital precoder design subproblems, and proposes hybrid precoding algorithm MBCD-HP based on modified form of BCD. We propose another hybrid precoding algorithm IPM-HP based on iterative power method in Section IV. In Section V, the proposed algorithms are extended for wideband MIMO-OFDM channel. Section VI is dedicated for the complexity evaluation of the proposed methods, and comparison with the existing methods. The simulation results are presented in Section VII, followed by the conclusion of our work in Section VIII.

B. NOTATIONS

$\mathbf{x}$ represents a vector, whereas $\mathbf{X}$ represents a matrix; $i{:}j$ represents all the integers from i to j, *i.e.*, $i{:}j = \{i, i+1, \ldots, j-1, j\}$; $\mathbf{X}_{i,j}$ and $\mathbf{X}_{,j}$ represent the $(i,j)^{th}$ element and the j^{th} column of $\mathbf{X}$ respectively; $\mathbf{X}_{i^c,j}$ is the j^{th} column of matrix $\mathbf{X}$ with i^{th} row removed, while $\mathbf{X}_{i,j^c}$ is the i^{th} row of matrix $\mathbf{X}$ with j^{th} column removed; $\mathbf{X}_{a:b,m:n}$ is a submatrix of $\mathbf{X}$ with rows a to b and columns m to n; $\|\mathbf{X}\|_F$ is the Frobenius norm of $\mathbf{X}$; $\mathbf{Tr}[\mathbf{X}]$ is the trace of $\mathbf{X}$; $\exp(\mathbf{X})$ is a matrix whose $(i,j)^{th}$ entry is $\exp\left(\mathbf{X}_{i,j}\right)$, where $\exp(.)$ is the exponential operator; $\mathbf{X}^{\dagger}$ and $\mathbf{X}^{H}$ are the pseudoinverse and Hermitian transpose of $\mathbf{X}$ respectively; $\mathbf{X} \in \mathbf{H}_p$ means that $\mathbf{X}$ lies in the cone of Hermitian matrices of dimension p; $\mathbf{diag}(\mathbf{X})$ is a column vector containing the diagonal elements of $\mathbf{X}$; $\mathbf{1}_{m\times n}$ is an $m \times n$ matrix with all elements equal to 1.

II. SYSTEM MODEL AND PROBLEM STATEMENT

In this section, we describe the system and channel we consider to model the mmWave MIMO system. We also state the hybrid precoding problem we intend to solve.

A. SYSTEM MODEL

We consider a single user mmWave MIMO downlink system in which the transmitter is equipped with N_t transmit antennas and M_t RF chains, whereas the receiver has N_r receive antennas and M_r RF chains. The number of data streams being transmitted is N_s. We assume $N_s \leq M_t \leq N_t$, $N_s \leq M_r \leq N_r$. We consider fully-connected architecture at both the transmitter and the receiver in which each RF chain is connected to all the antennas through a network of phase shifters.

At the transmitter, transmit signal is precoded by the hybrid precoder $\mathbf{F} = \mathbf{F}_{\mathrm{R}}\mathbf{F}_{\mathrm{D}}$ before transmission which is a combination of baseband precoder $\mathbf{F}_{\mathrm{D}} \in \mathbb{C}^{M_t\times N_s}$ and the analog beamformer $\mathbf{F}_{\mathrm{R}} \in \mathbb{C}^{N_t\times M_t}$. At the receiver, the received signal is processed by the hybrid combiner $\mathbf{W} = \mathbf{W}_{\mathrm{R}}\mathbf{W}_{\mathrm{D}}$ where $\mathbf{W}_{\mathrm{R}} \in \mathbb{C}^{N_r\times M_r}$ is the analog combiner and $\mathbf{W}_{\mathrm{D}} \in \mathbb{C}^{M_r\times N_s}$ is the digital combiner.

The analog beamformer and combiner are implemented using phase shifters which impose a constant unit amplitude constraint on each element of $\mathbf{F}_{\mathrm{R}}$ and $\mathbf{W}_{\mathrm{R}}$, *i.e.*, $|\mathbf{F}_{\mathrm{R}_{i,j}}| = 1$ and $|\mathbf{W}_{\mathrm{R}_{i,j}}| = 1$. We assume that all the transmit symbols are independent of each other such that $\mathbb{E}\left[\mathbf{s}\mathbf{s}^H\right] = \frac{1}{N_s}\mathbf{I}_{N_s}$. The hybrid precoder $\mathbf{F}$ is constrained to satisfy total power constraint so that the transmit signal does not exceed the total power limit, whereas the hybrid combiner $\mathbf{W}$ need not satisfy any power constraint.

We adopt narrow-band block-fading channel model in this paper similar to [11]. The received signal, after combining, is given by

$$\mathbf{y} = \sqrt{\rho}\mathbf{W}_{\mathrm{D}}^H\mathbf{W}_{\mathrm{R}}^H\mathbf{H}\mathbf{F}_{\mathrm{R}}\mathbf{F}_{\mathrm{D}}\mathbf{s} + \mathbf{W}_{\mathrm{D}}^H\mathbf{W}_{\mathrm{R}}^H\mathbf{n}, \tag{1}$$

where ρ is the average received power. $\mathbf{H} \in \mathbb{C}^{N_r\times N_t}$ is the channel from the transmitter to the receiver and $\mathbf{n}_k \sim \mathcal{CN}\left(\mathbf{0}, \sigma^2\mathbf{I}_{N_r}\right)$ is the $N_r \times 1$ complex noise vector.

B. CHANNEL MODEL

A clustered channel model based on extended Saleh Valenzuela model is considered to model mmWave channel so as to capture its scattering nature mathematically where we assume the channel matrix to be sum total of the contributions of a number of scatterers, each contributing a number of propagation paths [11]. The narrowband downlink channel

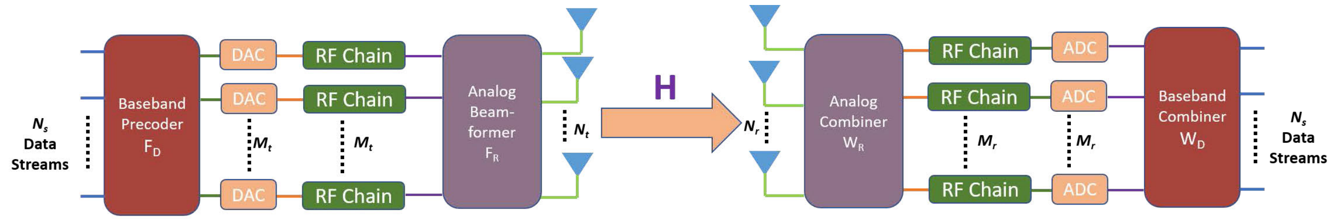

FIGURE 1. System diagram showing mmWave single user MIMO system with hybrid precoding at the transmitter and hybrid combining at the receiver.

between the transmitter and the receiver is given by

$$\mathbf{H} = \sqrt{\frac{N_t N_r}{N_c N_p}} \sum_{i=1}^{N_c} \sum_{\ell=1}^{N_p} \alpha_{i\ell} \mathbf{a}_r(\phi_{i\ell}^r, \theta_{i\ell}^r) \mathbf{a}_t{}^H(\phi_{i\ell}^t, \theta_{i\ell}^t), \quad (2)$$

where N_c is the number of clusters, N_p is the number of paths in each cluster, $\alpha_{i\ell}$ is the complex gain, $\phi_{i\ell}^t$ ($\theta_{i\ell}^t$) and $\phi_{i\ell}^r$ ($\theta_{i\ell}^r$) are the azimuth (elevation) angles of departure (AoDs) and azimuth (elevation) angles of arrival (AoAs) respectively, $\mathbf{a}_r(\phi_{i\ell}^r, \theta_{i\ell}^r)$ and $\mathbf{a}_t(\phi_{i\ell}^t, \theta_{i\ell}^t)$ are the antenna array response vectors of the receiver and the transmitter respectively. The subscript "$i\ell$" indicates a parameter associated with ℓ^{th} path in i^{th} cluster. We consider uniform linear arrays (ULAs) at both the transmitter and the receiver. The antenna array response vector of the transmitter can be written as

$$\mathbf{a}_t(\phi_{i\ell}^t) = \frac{1}{\sqrt{N_t}} \left[1, e^{jpd\sin(\phi_{i\ell}^t)}, \ldots, e^{j(N_t-1)pd\sin(\phi_{i\ell}^t)}\right]^T, \quad (3)$$

where $p = (2\pi/\lambda)$, λ is the carrier wavelength, and d is the distance between antenna elements. We can write the antenna array response vector of the receiver in a similar fashion.

C. PROBLEM STATEMENT

As suggested in [11], the problem of designing precoder and combiner can be divided into two different sub-problems.The design of combiner follows the similar procedure as that of the precoder design except that the combiner need not satisfy any power constraint. From [11], it follows that the hybrid precoder is given by

$$\begin{aligned} &\underset{\mathbf{F}_\mathrm{R}, \mathbf{F}_\mathrm{D}}{\arg\min} && \left\| \mathbf{F}_\mathrm{opt} - \mathbf{F}_\mathrm{R}\mathbf{F}_\mathrm{D} \right\|_F^2 \\ &\text{s.t.} && \|\mathbf{F}_\mathrm{R}\mathbf{F}_\mathrm{D}\|_F^2 = N_s, \\ & && \left|\mathbf{F}_{\mathrm{R}_{i,j}}\right| = 1, \ \forall i, j, \end{aligned} \quad (4)$$

where $\mathbf{F}_\mathrm{opt} \in \mathbb{C}^{N_t \times N_s}$ is the optimal fully digital precoder. The optimal precoder and combiner are the matrices containing the right singular vectors and the left singular vectors of the channel matrix respectively, corresponding to the N_s largest singular values. If the singular value decomposition (SVD) of channel matrix is $\mathbf{H} = \mathbf{USV}^H$, the optimal precoder and combiner are formed of the leading N_s columns of $\mathbf{V}$ and $\mathbf{U}$ respectively. The non-convex nature of the second constraint in (4) makes it pretty difficult to solve and there is no known solution [11]. Hence the general trend is to decompose the hybrid precoding problem (4) into two separate sub-problems to determine analog precoder and digital precoder separately. We can express the objective function in (4) in terms of trace as,

$$\begin{aligned} &\left\| \mathbf{F}_\mathrm{opt} - \mathbf{F}_\mathrm{R}\mathbf{F}_\mathrm{D} \right\|_F^2 \\ &= \mathbf{Tr}\left[\left(\mathbf{F}_\mathrm{opt} - \mathbf{F}_\mathrm{R}\mathbf{F}_\mathrm{D}\right)\left(\mathbf{F}_\mathrm{opt} - \mathbf{F}_\mathrm{R}\mathbf{F}_\mathrm{D}\right)^H\right] \\ &= \mathbf{Tr}\left[\mathbf{F}_\mathrm{opt}\mathbf{F}_\mathrm{opt}^H - \mathbf{F}_\mathrm{R}\mathbf{F}_\mathrm{D}\mathbf{F}_\mathrm{opt}^H - \mathbf{F}_\mathrm{opt}\mathbf{F}_\mathrm{D}^H\mathbf{F}_\mathrm{R}^H + \mathbf{F}_\mathrm{R}\mathbf{F}_\mathrm{D}\mathbf{F}_\mathrm{D}^H\mathbf{F}_\mathrm{R}^H\right]. \end{aligned}$$

III. HYBRID PRECODING METHOD BASED ON MODIFIED BLOCK COORDINATE DESCENT METHOD

The first hybrid precoding method is based on alternating minimization technique in which we alternately optimize digital precoder and analog precoder, keeping the other fixed. We start with a feasible initial value of analog precoder and the digital precoder is determined, keeping analog precoder fixed. The analog precoder is designed, treating the digital precoder as a constant in the next stage. This procedure of determining digital precoder and analog precoder is repeated until we reach convergence.

A. DIGITAL PRECODER DESIGN

If analog precoder $\mathbf{F}_\mathrm{R}$ is known, we can evaluate digital precoder $\mathbf{F}_\mathrm{D}$ by solving the problem

$$\begin{aligned} \mathbf{F}_\mathrm{D}^\star = \ &\underset{\mathbf{F}_\mathrm{D}}{\arg\min} \ \mathbf{Tr}\Big[\mathbf{F}_\mathrm{opt}\mathbf{F}_\mathrm{opt}^H - \mathbf{F}_\mathrm{R}\mathbf{F}_\mathrm{D}\mathbf{F}_\mathrm{opt}^H - \mathbf{F}_\mathrm{opt}\mathbf{F}_\mathrm{D}^H\mathbf{F}_\mathrm{R}^H \\ &\qquad\qquad + \mathbf{F}_\mathrm{R}\mathbf{F}_\mathrm{D}\mathbf{F}_\mathrm{D}^H\mathbf{F}_\mathrm{R}^H\Big] \\ &\text{s.t.} \qquad \mathbf{Tr}\left(\mathbf{F}_\mathrm{D}^H\mathbf{F}_\mathrm{R}^H\mathbf{F}_\mathrm{R}\mathbf{F}_\mathrm{D}\right) = N_s, \end{aligned} \quad (5)$$

To solve (5), we form Lagrangian,

$$\begin{aligned} \mathcal{L} = \mathbf{Tr}\left[\mathbf{F}_\mathrm{opt}\mathbf{F}_\mathrm{opt}^H - \mathbf{F}_\mathrm{R}\mathbf{F}_\mathrm{D}\mathbf{F}_\mathrm{opt}^H - \mathbf{F}_\mathrm{opt}\mathbf{F}_\mathrm{D}^H\mathbf{F}_\mathrm{R}^H + \mathbf{F}_\mathrm{R}\mathbf{F}_\mathrm{D}\mathbf{F}_\mathrm{D}^H\mathbf{F}_\mathrm{R}^H\right] \\ + \lambda\left[\mathbf{Tr}\left(\mathbf{F}_\mathrm{D}^H\mathbf{F}_\mathrm{R}^H\mathbf{F}_\mathrm{R}\mathbf{F}_\mathrm{D}\right) - N_s\right], \end{aligned} \quad (6)$$

where $\lambda \in \mathbb{R}$ is the Lagrangian constant that needs to be determined. Differentiating (6) w.r.t $\mathbf{F}_\mathrm{D}$ and equating it to $\mathbf{0}$ gives

$$\mathbf{F}_\mathrm{D} = \frac{1}{(1+\lambda)}\left(\mathbf{F}_\mathrm{R}^H\mathbf{F}_\mathrm{R}\right)^{-1}\mathbf{F}_\mathrm{R}^H\mathbf{F}_\mathrm{opt} = \beta\tilde{\mathbf{F}}_\mathrm{D}, \quad (7a)$$

$$\text{where} \quad \tilde{\mathbf{F}}_\mathrm{D} = \left(\mathbf{F}_\mathrm{R}^H\mathbf{F}_\mathrm{R}\right)^{-1}\mathbf{F}_\mathrm{R}^H\mathbf{F}_\mathrm{opt} = \mathbf{F}_\mathrm{R}^\dagger\mathbf{F}_\mathrm{opt} \quad (7b)$$

is the un-normalized digital precoder and $\beta = \frac{1}{(1+\lambda)}$ is the normalization factor. To determine the value of β, we equate the derivative of (6) w.r.t λ to 0 and substitute the value of $\mathbf{F}_{\rm D}$ from (7a) in the resulting equation. The value of β is obtained as

$$\beta = \sqrt{\frac{N_s}{\mathbf{Tr}\left(\tilde{\mathbf{F}}_{\rm D}^H \mathbf{F}_{\rm R}^H \mathbf{F}_{\rm R} \tilde{\mathbf{F}}_{\rm D}\right)}}. \tag{8}$$

B. ANALOG PRECODER DESIGN BY MODIFIED BLOCK COORDINATE DESCENT METHOD

The authors in [20] (Lemma 1) prove that if we minimize the Euclidean distance between the optimal precoder and the un-normalized hybrid precoder, the normalization step performed at the end will still make the distance between the hybrid precoder and the optimal precoder sufficiently small. Hence, we can discard the power constraint in (4) for the time being, and just minimize the Euclidean distance between the optimal precoder and the un-normalized hybrid precoder. The normalization of the digital precoder can be performed after we have computed the analog precoder and the un-normalized digital precoder. Hence, if the digital precoder is known, the analog precoder design sub-problem can be restated as

$$\begin{aligned} \min_{\mathbf{F}_{\rm R}} \quad & \mathbf{Tr}\Big[\mathbf{F}_{\rm opt}\mathbf{F}_{\rm opt}^H - \mathbf{F}_{\rm R}\tilde{\mathbf{F}}_{\rm D}\mathbf{F}_{\rm opt}^H - \mathbf{F}_{\rm opt}\tilde{\mathbf{F}}_{\rm D}^H\mathbf{F}_{\rm R}^H \\ & \quad + \mathbf{F}_{\rm R}\tilde{\mathbf{F}}_{\rm D}\tilde{\mathbf{F}}_{\rm D}^H\mathbf{F}_{\rm R}^H\Big] \\ \text{s.t.} \quad & \left|\mathbf{F}_{{\rm R}_{i,j}}\right| = 1, \ \forall i,j, \end{aligned} \tag{9}$$

Discarding the term containing only $\mathbf{F}_{\rm opt}\mathbf{F}_{\rm opt}^H$ which does not depend on $\mathbf{F}_{\rm R}$, the analog precoding subproblem in (9) can be equivalently written as

$$\begin{aligned} \min_{\mathbf{F}_{\rm R}} \ & \mathbf{Tr}\Big[\mathbf{F}_{\rm R}\tilde{\mathbf{F}}_{\rm D}\tilde{\mathbf{F}}_{\rm D}^H\mathbf{F}_{\rm R}^H - \mathbf{F}_{\rm R}\tilde{\mathbf{F}}_{\rm D}\mathbf{F}_{\rm opt}^H - \mathbf{F}_{\rm opt}\tilde{\mathbf{F}}_{\rm D}^H\mathbf{F}_{\rm R}^H\Big] \\ \text{s.t.} \ & \left|\mathbf{F}_{{\rm R}_{i,j}}\right| = 1, \ \forall i,j. \end{aligned} \tag{10}$$

To solve the optimization problem in (10), we introduce another optimization problem,

$$\min_{\tilde{\mathbf{F}}_{\rm R}} \quad \mathbf{Tr}\left[\tilde{\mathbf{F}}_{\rm R}^H \mathbf{M} \tilde{\mathbf{F}}_{\rm R}\right], \quad \text{where} \tag{11a}$$

$$\mathbf{M} = \begin{bmatrix} \tilde{\mathbf{F}}_{\rm D}\tilde{\mathbf{F}}_{\rm D}^H & -\frac{1}{\sqrt{N_t}}\tilde{\mathbf{F}}_{\rm D}\mathbf{F}_{\rm opt}^H \\ -\frac{1}{\sqrt{N_t}}\mathbf{F}_{\rm opt}\tilde{\mathbf{F}}_{\rm D}^H & \mathbf{0} \end{bmatrix}, \tag{11b}$$

$$\tilde{\mathbf{F}}_{\rm R} = \begin{bmatrix} \bar{\mathbf{F}}_{\rm R}^H \\ \mathbf{I}_{\rm N_t} \end{bmatrix}, \quad |\bar{\mathbf{F}}_{\rm R}| = \frac{1}{\sqrt{N_t}}\mathbf{1}_{\rm N_t \times M_t}. \tag{11c}$$

If we expand the problem (11), we can easily see that it is equivalent to problem (10) with $\mathbf{F}_{\rm R} = \sqrt{N_t}\bar{\mathbf{F}}_{\rm R}$. If the optimal solution to (11) is $\tilde{\mathbf{F}}_{\rm R}^{\star} = \left[\left(\bar{\mathbf{F}}_{\rm R}^{\star H}\right)^T, \mathbf{I}_{\rm N_t}\right]^T$, it is obvious that the optimal solution of (10) is $\mathbf{F}_{\rm R}^{\star} = \sqrt{N_t}\bar{\mathbf{F}}_{\rm R}^{\star}$. Thus, we can solve problem (11) to determine the analog precoder.

We define the Hermitian matrix,

$$\mathbf{X} = \tilde{\mathbf{F}}_{\rm R}\tilde{\mathbf{F}}_{\rm R}^H = \begin{bmatrix} \bar{\mathbf{F}}_{\rm R}^H\bar{\mathbf{F}}_{\rm R} & \bar{\mathbf{F}}_{\rm R}^H \\ \bar{\mathbf{F}}_{\rm R} & \mathbf{I}_{\rm N_t} \end{bmatrix} \tag{12}$$

Since the i^{th} diagonal element of $\bar{\mathbf{F}}_{\rm R}^H\bar{\mathbf{F}}_{\rm R}$ is equal to the sum of squares of absolute values of all the elements of the i^{th} column of $\bar{\mathbf{F}}_{\rm R}$, it is evident that all the diagonal elements of $\bar{\mathbf{F}}_{\rm R}^H\bar{\mathbf{F}}_{\rm R}$ are equal to 1. Hence, it is easy to see that $\mathbf{diag}(\mathbf{X}) = \mathbf{1}_{m\times 1}$, where we define $m \triangleq (N_t + M_t)$. We also define $q \triangleq 1 : M_t$ and $r \triangleq (M_t + 1) : (N_t + M_t)$ Thus, the problem in (11) can be restated as

$$\begin{aligned} \min_{\mathbf{X}\in\mathbf{H}_{\rm m}} \quad & \mathbf{Tr}(\mathbf{MX}) \\ \text{s.t.} \quad & \mathbf{X} \succeq 0, \\ & \mathbf{diag}(\mathbf{X}) = \mathbf{1}_{m\times 1}, \\ & \left|\mathbf{X}_{r,q}\right| = \frac{1}{\sqrt{N_t}}\mathbf{1}_{N_t\times M_t} = \left|\mathbf{X}_{q,r}^H\right|, \quad \mathbf{X}_{r,r} = \mathbf{I}_{N_t}, \\ & \text{rank}(\mathbf{X}) = N_t. \end{aligned} \tag{13}$$

We let go of the non-convex rank constraint to achieve convex relaxation,

$$\min_{\mathbf{X}\in\mathbf{H}_{\rm m}} \quad \mathbf{Tr}(\mathbf{MX}) \tag{14a}$$

$$\text{s.t.} \quad \mathbf{X} \succeq 0, \tag{14b}$$

$$\mathbf{diag}(\mathbf{X}) = \mathbf{1}_{m\times 1}, \tag{14c}$$

$$\left|\mathbf{X}_{r,q}\right| = \frac{1}{\sqrt{N_t}}\mathbf{1}_{N_t\times M_t} = \left|\mathbf{X}_{q,r}^H\right|, \quad \mathbf{X}_{r,r} = \mathbf{I}_{N_t}. \tag{14d}$$

The problem (14) is a semi-definite programming (SDP) in $\mathbf{X}$. The problem in (14) looks similar to *PhaseCut*, the phase retrieval problem formulated as an SDP after a tractable convex relaxation [26] except for the additional last constraint in (14d).

We can choose among the numerous efficient algorithms to solve PhaseCut problem and use it to determine the unknown $\mathbf{X}$ in (14). However, we need to integrate the constraint (14d) in the chosen method as it does not exist in the standard PhaseCut problems. We choose Block Coordinate Descent (BCD) algorithm [27] and modify it to incorporate the additional constraint (14d) to solve (14) and propose what we call *modified Block Coordinate Descent (MBCD)* algorithm that takes account of the structure of $\mathbf{X}$. The proposed MBCD algorithm is summed up in Algorithm 1. The proposed MBCD algorithm is exactly same as the BCD algorithm [26] except for the step 9 that ensures the constraint (14d) is incorporated.

In the phase retrieval problem, the final aim is to find column vector $\mathbf{v}$ such that $\mathbf{v}\mathbf{v}^H = \mathbf{X}$ which is usually determined by normalizing each entry of the leading SVD vector or eigenvector of matrix $\mathbf{X}$ to have magnitude of 1 [26]. However, we are solving the problem (14) for $\mathbf{X} = \tilde{\mathbf{F}}_{\rm R}\tilde{\mathbf{F}}_{\rm R}^H$ where $\tilde{\mathbf{F}}_{\rm R}$ is a $(N_t + M_t) \times N_t$ matrix, not a vector. However, we can exploit the structure of $\mathbf{X}$ revealed in (12) to obtain $\bar{\mathbf{F}}_{\rm R}$ and hence, $\mathbf{F}_{\rm R}$ directly from $\mathbf{X}$ as prosecuted in step 5 of Algorithm 2. We can observe from (12) that the submatrix corresponding to the last N_t rows and the first M_t columns of $\mathbf{X}$ is equal to $\bar{\mathbf{F}}_{\rm R}$. Thus, we can directly compute $\mathbf{F}_{\rm R} = \sqrt{N_t}\bar{\mathbf{F}}_{\rm R}$ from $\mathbf{X}$.

Algorithm 1 Modified Block Coordinate Descent (MBCD) Algorithm

Require: $\mathbf{M}$, M_t, feasible initial $n \times n$ matrix $\mathbf{X}^1$.
Choose $\nu > 0$ such that $\nu \to 0$ and integer $N_{it}^i > 1$.
for $k = 1, \ldots, N_{it}^i$ **do**
  Pick $i \in [1, n]$.
  Compute $\mathbf{Y} = \mathbf{X}^k_{i^c,i^c}\mathbf{M}_{i^c,i}$.
  Compute $\zeta = \mathbf{Re}\left(\mathbf{Y}^H\mathbf{M}_{i^c,i}\right)$.
  if $\zeta > 0$ **then**
    $\mathbf{X}^{k+1}_{i^c,i} = \mathbf{X}^{k+1^H}_{i,i^c} = -\sqrt{\frac{1-\nu}{\zeta}}\mathbf{Y}$
  else
    $\mathbf{X}^{k+1}_{i^c,i} = \mathbf{X}^{k+1^H}_{i,i^c} = 0$
  end if
  $\mathbf{X}^{k+1}_{r,r} = \mathbf{I}_{N_t}$ and $\mathbf{X}^{k+1}_{r,q} = \mathbf{X}^{k+1^H}_{q,r} = \frac{1}{\sqrt{N_t}}\exp(j\angle\mathbf{X}^{k+1}_{r,q})$, where $q = 1 : M_t$ and $r = M_t + 1 : n$.
end for
return $\mathbf{X}$.

This way we can circumvent the use of computationally expensive SVD operation on $\mathbf{X}$.

C. HYBRID PRECODER DESIGN VIA ALTERNATING MINIMIZATION

In the proposed hybrid precoding method that we call MBCD-HP, we use alternating minimization technique to determine hybrid precoder. We begin with a feasible initial value of analog precoder $\mathbf{F}_{\mathrm{R}}^{(0)}$. The iteration index k is set to 1. At each iteration k, we determine digital precoder $\tilde{\mathbf{F}}_{\mathrm{D}}^{k}$ as $\mathbf{F}_{\mathrm{R}}^{(k-1)^\dagger}\mathbf{F}_{\mathrm{opt}}$. $\mathbf{M}^k$ is determined using (11b) and we update the value of $\mathbf{F}_{\mathrm{R}}^{(k)}$ using Algorithm 1. The iteration index k is increased by 1. The procedure of determining $\tilde{\mathbf{F}}_{\mathrm{D}}$ and $\mathbf{F}_{\mathrm{R}}$ alternately is repeated until the convergence or the maximum number of iterations is reached. The algorithm has been summarized in Algorithm 2.

IV. HYBRID PRECODER BASED ON ITERATIVE POWER METHOD

While using the MBCD-HP algorithm, we need to compute the unconstrained digital precoder and analog precoder using MBCD algorithm at each iteration which adds to the complexity. In a bid to reduce the complexity further, we propose a hybrid precoder based on iterative power method that gets rid of the burden of computing digital precoder and analog precoder at each iteration. We substitute the expression for $\tilde{\mathbf{F}}_{\mathrm{D}}$ from (7) in the objective function in (10) and with valid assumptions simplify it to obtain the analog precoding subproblem. The objective function in (10) can be written as

$$\begin{aligned}
&\mathbf{Tr}\left[\mathbf{F}_{\mathrm{R}}\tilde{\mathbf{F}}_{\mathrm{D}}\tilde{\mathbf{F}}_{\mathrm{D}}^H\mathbf{F}_{\mathrm{R}}^H - \mathbf{F}_{\mathrm{R}}\tilde{\mathbf{F}}_{\mathrm{D}}\mathbf{F}_{\mathrm{opt}}^H - \mathbf{F}_{\mathrm{opt}}\tilde{\mathbf{F}}_{\mathrm{D}}^H\mathbf{F}_{\mathrm{R}}^H\right]\\
&\overset{(a)}{\approx} \mathbf{Tr}\left[\frac{1}{N_t^2}\mathbf{F}_{\mathrm{R}}\mathbf{F}_{\mathrm{R}}^H\mathbf{F}_{\mathrm{opt}}\mathbf{F}_{\mathrm{opt}}^H\mathbf{F}_{\mathrm{R}}\mathbf{F}_{\mathrm{R}}^H - \frac{1}{N_t}\mathbf{F}_{\mathrm{R}}\mathbf{F}_{\mathrm{R}}^H\mathbf{F}_{\mathrm{opt}}\mathbf{F}_{\mathrm{opt}}^H \right.\\
&\qquad\left. - \frac{1}{N_t}\mathbf{F}_{\mathrm{opt}}\mathbf{F}_{\mathrm{opt}}^H\mathbf{F}_{\mathrm{R}}\mathbf{F}_{\mathrm{R}}^H\right]\\
&\overset{(b)}{\approx} \frac{1}{N_t}\mathbf{Tr}\left[\mathbf{F}_{\mathrm{R}}^H\mathbf{F}_{\mathrm{opt}}\mathbf{F}_{\mathrm{opt}}^H\mathbf{F}_{\mathrm{R}}\right] - \mathbf{Tr}\left[\frac{1}{N_t}\mathbf{F}_{\mathrm{R}}\mathbf{F}_{\mathrm{R}}^H\mathbf{F}_{\mathrm{opt}}\mathbf{F}_{\mathrm{opt}}^H \right.\\
&\qquad\left. + \frac{1}{N_t}\mathbf{F}_{\mathrm{opt}}\mathbf{F}_{\mathrm{opt}}^H\mathbf{F}_{\mathrm{R}}\mathbf{F}_{\mathrm{R}}^H\right]\\
&= -\mathbf{Tr}\left[\frac{1}{N_t}\mathbf{F}_{\mathrm{R}}\mathbf{F}_{\mathrm{R}}^H\mathbf{F}_{\mathrm{opt}}\mathbf{F}_{\mathrm{opt}}^H\right],
\end{aligned}$$

Algorithm 2 Alternating Minimization Hybrid Precoding Algorithm Based on Modified Block Coordinate Descent Method

Require: $\mathbf{F}_{\mathrm{opt}}$, N_t, M_t.
Set initial $\mathbf{F}_{\mathrm{R}}^{(0)}$ such that $\left|\mathbf{F}_{\mathrm{R}}^{(0)}\right| = \mathbf{1}_{N_t \times M_t}$ and set $k = 1$.
repeat
  Compute $\tilde{\mathbf{F}}_{\mathrm{D}}^{(k)} = \mathbf{F}_{\mathrm{R}}^{(k-1)^\dagger}\mathbf{F}_{\mathrm{opt}}$.
  Compute $\mathbf{M}^{(k)}$ using (11b) and determine $\mathbf{X}^{(k)}$ with the help of Algorithm 1.
  Compute $\mathbf{F}_{\mathrm{R}}^{(k)} = \sqrt{N_t}\mathbf{X}^{(k)}_{r,q}$ where $r = M_t + 1 : N_t + M_t$ and $q = 1 : M_t$.
  $\delta^k = \left|f^k - f^{k-1}\right|$, where $f^k = \left\|\mathbf{F}_{\mathrm{opt}} - \mathbf{F}_{\mathrm{R}}^{(k)}\tilde{\mathbf{F}}_{\mathrm{D}}^{(k)}\right\|_F^2$.
  $k \leftarrow k + 1$.
until $\delta^k < \epsilon$ where $\epsilon \to 0$, or $k \geq max$, the maximum number of iterations.
Set $\mathbf{F}_{\mathrm{R}} = \mathbf{F}_{\mathrm{R}}^{(k)}$, $\tilde{\mathbf{F}}_{\mathrm{D}} = \tilde{\mathbf{F}}_{\mathrm{D}}^{(k)}$.
Calculate $\mathbf{F}_{\mathrm{D}} = \beta\tilde{\mathbf{F}}_{\mathrm{D}}$, where β is calculated using (8).
return $\mathbf{F} = \mathbf{F}_{\mathrm{R}}\mathbf{F}_{\mathrm{D}}$.

where the reasons behind (a): $\tilde{\mathbf{F}}_{\mathrm{D}} = \mathbf{F}_{\mathrm{R}}^\dagger\mathbf{F}_{\mathrm{opt}} \approx \frac{1}{N_t}\mathbf{F}_{\mathrm{R}}^H\mathbf{F}_{\mathrm{opt}}$ as $\mathbf{F}_{\mathrm{R}}^H\mathbf{F}_{\mathrm{R}} \approx N_t\mathbf{I}$ in mmWave MIMO as $N_t \to \infty$ [11], (b): $\mathbf{Tr}\,[\mathbf{AB}] = \mathbf{Tr}\,[\mathbf{BA}]$ and $\mathbf{F}_{\mathrm{R}}^H\mathbf{F}_{\mathrm{R}} \approx N_t\mathbf{I}$. Thus, the analog precoding subproblem can be equivalently written as

$$\max_{\mathbf{F}_{\mathrm{R}}} \quad \frac{1}{N_t}\mathbf{Tr}\left[\mathbf{F}_{\mathrm{R}}^H\left(\mathbf{F}_{\mathrm{opt}}\mathbf{F}_{\mathrm{opt}}^H\right)\mathbf{F}_{\mathrm{R}}\right]. \tag{15}$$

If we define $\bar{\mathbf{F}}_{\mathrm{R}} = \frac{1}{\sqrt{N_t}}\mathbf{F}_{\mathrm{R}}$, the analog precoding subproblem can be equivalently represented by

$$\max_{\bar{\mathbf{F}}_{\mathrm{R}}} \quad \mathbf{Tr}\left[\bar{\mathbf{F}}_{\mathrm{R}}^H\left(\mathbf{F}_{\mathrm{opt}}\mathbf{F}_{\mathrm{opt}}^H\right)\bar{\mathbf{F}}_{\mathrm{R}}\right] \tag{16a}$$

$$\text{s.t.} \quad \left|\bar{\mathbf{F}}_{\mathrm{R}_{i,j}}\right| = \frac{1}{\sqrt{N_t}}, \ \forall i, j, \tag{16b}$$

$$\bar{\mathbf{F}}_{\mathrm{R}}^H\bar{\mathbf{F}}_{\mathrm{R}} = \mathbf{I}_{M_t}, \tag{16c}$$

where we have added an extra orthogonal constraint (16c) on $\bar{\mathbf{F}}_{\mathrm{R}}$ which implies the constraint $\mathbf{F}_{\mathrm{R}}^H\mathbf{F}_{\mathrm{R}} = N_t\mathbf{I}$ on $\mathbf{F}_{\mathrm{R}}$ which is a fair constraint in mmWave MIMO. If it were not for the constraint (16b) in problem (16), the solution would be given by the matrix containing the M_t leading eigenvectors of $\mathbf{F}_{\mathrm{opt}}\mathbf{F}_{\mathrm{opt}}^H$. So, we propose a solution based on iterative power method to solve (16). Similar iterative power method is used in the computation of eigenvectors [28]. However, the proposed iterative power method is modified to make sure that the solution satisfies the constraint (16b) at each iteration.

In the proposed method based on iterative power method, we start with a feasible $\bar{\mathbf{F}}_{\mathrm{R}}^{(0)}$ and set iteration index k

to 1. At each iteration k, we form a product matrix $\left(\mathbf{F}_{\text{opt}}\mathbf{F}_{\text{opt}}^{H}\right)\bar{\mathbf{F}}_{\text{R}}^{(k-1)}$. We make sure that the columns of the product matrix are orthogonal to each other and also satisfy the constraint (16b) to produce $\bar{\mathbf{F}}_{\text{R}}^{(k)}$. The iteration index k is increased by 1. This procedure is repeated until convergence or we reach maximum number of iterations. The analog precoder $\mathbf{F}_{\text{R}}$ is computed as $\mathbf{F}_{\text{R}} = \sqrt{N_t}\bar{\mathbf{F}}_{\text{R}}^{(k)}$ and $\mathbf{F}_{\text{D}}$ can be determined using (7). The hybrid precoding algorithm based on iterative power method is given in Algorithm 3. We use modified Gram-Schmidt (MGS) procedure [29] to implement orthogonality constraint (16c) on $\bar{\mathbf{F}}_{\text{R}}$. However, we also need to accommodate the constraint (16b) on $\bar{\mathbf{F}}_{\text{R}}$. Hence, we have adapted the MGS algorithm in order that each column of the output matrix $\mathbf{Q}_{m\times n}$ is normalized so that its each element has constant modulus of $\frac{1}{\sqrt{m}}$ and name it adapted modified Gram-Schmidt (AMGS) orthogonalization procedure. The AMGS procedure is provided in Algorithm 4. Obviously, the analog precoder $\mathbf{F}_{\text{R}}$ computed using AMGS procedure is not going to be exactly orthogonal but only approximately orthogonal as the output matrix $\mathbf{Q}$ of Algorithm 4 is derived by extracting only the phases of an orthogonal matrix. However, it works as good substitute as there is no method to the authors' knowledge to determine the matrix in which each element satisfies constant modulus constraint and the columns are orthogonal to each other from a given matrix.

Algorithm 3 Iterative Power Method Based Hybrid Precoding Algorithm

Require: $\mathbf{F}_{\text{opt}}, M_t$.
- Compute $\mathbf{M} = \mathbf{F}_{\text{opt}}\mathbf{F}_{\text{opt}}^{H}$.
- Set initial $\bar{\mathbf{F}}_{\text{R}}^{(0)}$ such that $\left|\bar{\mathbf{F}}_{\text{R}}^{(0)}\right| = \frac{1}{\sqrt{N_t}}\mathbf{1}_{N_t\times M_t}$ and set $k = 1$.
- **repeat**
  - Perform the adapted Modified Gram-Schmidt orthogonalization procedure on $\mathbf{M}\bar{\mathbf{F}}_{\text{R}}^{(k-1)}$ to compute $\bar{\mathbf{F}}_{\text{R}}^{(k)}$, using Algorithm 4.
  - $\delta^k = \left|f^k - f^{k-1}\right|$, where $f^k = \mathbf{Tr}\left[\bar{\mathbf{F}}_{\text{R}}^{(k)^H}\mathbf{M}\bar{\mathbf{F}}_{\text{R}}^{(k)}\right]$.
  - $k \leftarrow k+1$.
- **until** $\delta^k < \epsilon$ where $\epsilon \to 0$, or $k \geq max$, the maximum number of iterations.
- Set $\mathbf{F}_{\text{R}} = \sqrt{N_t}\bar{\mathbf{F}}_{\text{R}}^{(k)}$. Compute $\tilde{\mathbf{F}}_{\text{D}} = \mathbf{F}_{\text{R}}^{\dagger}\mathbf{F}_{\text{opt}}$.
- Calculate $\mathbf{F}_{\text{D}} = \beta\tilde{\mathbf{F}}_{\text{D}}$, where β is calculated using (8).
- **return** $\mathbf{F} = \mathbf{F}_{\text{R}}\mathbf{F}_{\text{D}}$.

V. HYBRID PRECODING FOR WIDEBAND CHANNEL

In the previous section, we considered narrowband mmWave channel and proposed hybrid precoding methods for the same. However, the mmWave channel equipped with the large bandwidth exhibits frequency selectivity and multi-path fading. Similar to [20], [21], we consider orthogonal frequency division multiplexing (OFDM) is employed in the wideband channel and propose hybrid precoders for

Algorithm 4 Adapted Modified Gram-Schmidt (AMGS) Orthogonalization Procedure

Require: $\mathbf{X}_{m\times n}$.
- Initialize $\mathbf{Q} = \mathbf{0}_{m\times n}$.
- **for** $j = 1, \ldots, n$ **do**.
  - $\mathbf{v} = \mathbf{X}_{.j}$
  - **for** $i = 1, \ldots, j-1$ **do**
    - $r_{ij} = \mathbf{Q}_{.i}^{H}\mathbf{v}$
    - $\mathbf{v} = \mathbf{v} - r_{ij}\mathbf{Q}_{.i}$
  - **end for**
  - Compute $\mathbf{Q}_{.j} = \frac{1}{\sqrt{m}}\exp\left(j\angle\mathbf{v}\right)$.
- **end for**
- **return** $\mathbf{Q}$

mmWave MIMO-OFDM systems, using the developments made for narrowband channel. The mmWave MIMO-OFDM channel for the s^{th} sub-carrier is [20]

$$\mathbf{H}[s] = \sqrt{\frac{N_tN_r}{N_cN_p}}\sum_{i=0}^{N_c-1}\sum_{\ell=1}^{N_p}\alpha_{i\ell}\mathbf{a}_r(\theta_{i\ell}^{r},\phi_{i\ell}^{r})\mathbf{a}_t{}^{H}(\theta_{i\ell}^{t},\phi_{i\ell}^{t})\, e^{(-j2\pi is/S_c)}, \quad (17)$$

where S_c is the number of subcarriers and $s \in [0, S_c-1]$ is the sub-carrier index. In the conventional MIMO-OFDM, the digital precoding is performed for each subcarrier, which is followed by inverse fast Fourier Transform (IFFT) that sums all the subcarrier signals together. The mmWave MIMO-OFDM espouses similar procedure with the additional analog precoding succeeding the IFFT operation [20]. Hence, even though there are different digital precoding matrices for each sub-carrier, the analog precoding matrix is common for all sub-carriers. Hence, the received signal on the s^{th} subcarrier after combining process is given by

$$\mathbf{y}[s] = \sqrt{\rho}\mathbf{W}_{\text{D}}^{H}[s]\mathbf{W}_{\text{R}}^{H}\mathbf{H}[s]\mathbf{F}_{\text{R}}\mathbf{F}_{\text{D}}[s]\mathbf{s} + \mathbf{W}_{\text{D}}^{H}[s]\mathbf{W}_{\text{R}}^{H}\mathbf{n}, \quad (18)$$

where $\mathbf{W}_{\text{D}}[s]$ and $\mathbf{F}_{\text{D}}[s]$ are the digital parts of the hybrid combiner and hybrid precoder respectively, for the s^{th} subcarrier. The hybrid precoding problem for mmWave MIMO-OFDM can be written as [20], [30]

$$\begin{aligned}\min_{\mathbf{F}_{\text{R}},\mathbf{F}_{\text{D}}[s]} \quad & \sum_{s=0}^{S_c-1}\left\|\mathbf{F}_{\text{opt}}[s] - \mathbf{F}_{\text{R}}\mathbf{F}_{\text{D}}[s]\right\|_F^2 \\ \text{s.t.} \quad & \|\mathbf{F}_{\text{R}}\mathbf{F}_{\text{D}}[s]\|_F^2 = N_s, \\ & \left|\mathbf{F}_{\text{R}_{i,j}}\right| = 1,\ \forall i,j, \end{aligned} \quad (19)$$

where $\mathbf{F}_{\text{opt}}[s]$ is the optimal fully digital precoder for the s^{th} subcarrier.

A. HYBRID PRECODER BASED ON MODIFIED BLOCK COORDINATE DESCENT FOR mmWave MIMO-OFDM

For the modified BCD-based algorithm, we can write the analog precoding problem for the MIMO-OFDM, similar to that in (10), as

$$\begin{aligned}\min_{\mathbf{F}_\mathrm{R}} \quad & \sum_{s=0}^{S_c-1} \mathbf{Tr}\Big[\mathbf{F}_\mathrm{R}\tilde{\mathbf{F}}_\mathrm{D}[s]\tilde{\mathbf{F}}_\mathrm{D}^H[s]\mathbf{F}_\mathrm{R}^H - \mathbf{F}_\mathrm{R}\tilde{\mathbf{F}}_\mathrm{D}[s]\mathbf{F}_\mathrm{opt}^H[s] \\ & \quad - \mathbf{F}_\mathrm{opt}[s]\tilde{\mathbf{F}}_\mathrm{D}^H[s]\mathbf{F}_\mathrm{R}^H\Big] \\ \text{s.t.} \quad & \left|\mathbf{F}_{\mathrm{R}_{i,j}}\right| = 1, \ \forall i, j. \end{aligned} \tag{20}$$

The objective function of the problem (20) can be written as

$$\mathbf{Tr}\left[\mathbf{F}_\mathrm{R}\left(\sum_{s=0}^{S_c-1}\tilde{\mathbf{F}}_\mathrm{D}[s]\tilde{\mathbf{F}}_\mathrm{D}^H[s]\right)\mathbf{F}_\mathrm{R}^H - \mathbf{F}_\mathrm{R}\left(\sum_{s=0}^{S_c-1}\tilde{\mathbf{F}}_\mathrm{D}[s]\mathbf{F}_\mathrm{opt}^H[s]\right) - \left(\sum_{s=0}^{S_c-1}\mathbf{F}_\mathrm{opt}[s]\tilde{\mathbf{F}}_\mathrm{D}^H[s]\right)\mathbf{F}_\mathrm{R}^H\right]. \tag{21}$$

Thus, the analog precoder for mmWave MIMO-OFDM has been translated into optimization problem similar to that for the narrowband channel in (10) and hence solved by the same alternating minimization algorithm as in Algorithm 2. At each iteration, matrix $\mathbf{M}$ and the unconstrained digital precoder matrix for the s^{th} subcarrier, $\tilde{\mathbf{F}}_\mathrm{D}[s]$ can be determined as

$$\mathbf{M} = \begin{bmatrix} \sum_s \tilde{\mathbf{F}}_\mathrm{D}[s]\tilde{\mathbf{F}}_\mathrm{D}^H[s] & -\frac{1}{\sqrt{N_t}}\sum_s \tilde{\mathbf{F}}_\mathrm{D}[s]\mathbf{F}_\mathrm{opt}^H[s] \\ -\frac{1}{\sqrt{N_t}}\sum_s \mathbf{F}_\mathrm{opt}[s]\tilde{\mathbf{F}}_\mathrm{D}^H[s] & \mathbf{0} \end{bmatrix}$$

$$\tilde{\mathbf{F}}_\mathrm{D}[s] = \mathbf{F}_\mathrm{R}^\dagger\mathbf{F}_\mathrm{opt}[s] \tag{22}$$

B. HYBRID PRECODER BASED ON ITERATIVE POWER METHOD FOR mmWave MIMO-OFDM

The mmWave MIMO-OFDM analog precoding problem equivalent to its narrowband counterpart in (16) can be written as

$$\begin{aligned}\max_{\bar{\mathbf{F}}_\mathrm{R}} \quad & \sum_{s=0}^{S_c-1}\mathbf{Tr}\left[\bar{\mathbf{F}}_\mathrm{R}^H\left(\mathbf{F}_\mathrm{opt}[s]\mathbf{F}_\mathrm{opt}^H[s]\right)\bar{\mathbf{F}}_\mathrm{R}\right] \\ \text{s.t.} \quad & \text{(16b)} \quad \text{and} \quad \text{(16c)}, \end{aligned} \tag{23}$$

which is equivalent to

$$\begin{aligned}\max_{\bar{\mathbf{F}}_\mathrm{R}} \quad & \mathbf{Tr}\left[\bar{\mathbf{F}}_\mathrm{R}^H\left(\sum_{s=0}^{S_c-1}\mathbf{F}_\mathrm{opt}[s]\mathbf{F}_\mathrm{opt}^H[s]\right)\bar{\mathbf{F}}_\mathrm{R}\right] \\ \text{s.t.} \quad & \text{(16b)} \quad \text{and} \quad \text{(16c)}. \end{aligned} \tag{24}$$

We can solve for $\mathbf{F}_\mathrm{R} = \sqrt{N_t}\bar{\mathbf{F}}_\mathrm{R}$ by solving (24) using the Algorithm 3 where $\mathbf{M} = \sum_{s=0}^{S_c-1}\mathbf{F}_\mathrm{opt}[s]\mathbf{F}_\mathrm{opt}^H[s]$. The digital precoder and then the hybrid precoder for each subcarrier can be determined subsequently.

VI. COMPLEXITY ANALYSES OF THE PROPOSED METHODS

The complexity of the hybrid precoding algorithm is mainly governed by the computation of its analog precoder. We compare the computational complexities of calculating analog precoder of the proposed methods with several existing hybrid precoding algorithms. We compute the complexities of the proposed algorithms in narrowband scenario and list the complexities of the algorithms for both the narrowband and the wideband scenarios in TABLE 1. It is worth mentioning that we have ignored the complexity in computing optimal fully digital precoder. All the algorithms under consideration require fully digital optimal precoder and their respective computational complexities do not consider the complexity incurred in computing optimal precoder. In TABLE 1, also listed are the complexities of several existing precoders HD-LSR, SSP, MO-AltMin and SDR-AO in narrowband case. The complexity of MO-AltMin has been sourced from [21], whereas the complexity of SSP have been derived from [24].

TABLE 1. Comparison of computational complexity of different Algorithms.

Narrowband	
Algorithm	**Complexity**
HD-LSR [18]	$\mathcal{O}\left(N_{it}\left(N_tM_tN_s + N_tN_s^2\right)\right)$
SSP [11]	$\mathcal{O}\left(N_t^2M_tN_s\right)$
MO-AltMin [20]	$N_{it}^oN_{it}^i\mathcal{O}\left(4N_t^2M_t + 13N_tM_t^2 + 3N_tM_t + 8M_t^3\right)$
SDR-AO [24]	$\mathcal{O}\left(N_{it}\left(M_t^7\left(N_t^7 + N_s^7\right) + M_t^3\left(N_t^3 + N_s^3\right)\right)\right)$
MBCD-HP	$N_{it}^o\mathcal{O}\left(N_{it}^i\left(N_t + M_t - 1\right)^2 + N_t^2M_t + 2N_tM_tN_s + M_t^2N_s\right)$
IPM-HP	$\mathcal{O}\left(N_{it}N_t^2M_t + N_tM_t^2 + N_t^2N_s\right)$
Wideband	
Algorithm	**Complexity**
MBCD-HP	$N_{it}^o\mathcal{O}\left(N_{it}^i\left(N_t + M_t - 1\right)^2 + N_t^2M_t + 2S_cN_tM_tN_s + M_t^2N_s\right)$
IPM-HP	$\mathcal{O}\left(N_{it}N_t^2M_t + N_tM_t^2 + S_cN_t^2N_s\right)$

The complexity of MBCD-HP at each iteration k is mainly governed by the modified BCD algorithm and the computation of $\tilde{\mathbf{F}}_\mathrm{D}^{(k)}$ which involves pseudoinverse computation of $\mathbf{F}_\mathrm{R}^{(k-1)}$ and a matrix multiplication. The complexity of BCD algorithm can not be categorically evaluated [26]. However, we attempt to estimate the complexity of the modified BCD algorithm in the worst case scenario. The complexity of the modified BCD algorithm mainly depends on step 4 of the Algorithm 1 which has the complexity of $\mathcal{O}\left((n-1)^2\right)$. The size of matrix $\mathbf{M}^{(k)}$ which is the input to modified BCD algorithm is $N_t + M_t$ so that $n = N_t + M_t$ and the step 4 in Algorithm 1 is repeated N_{it}^i times. The computation of pseudoinverse of $\mathbf{F}_\mathrm{R}^{(k-1)}$ involves a complexity of $\mathcal{O}\left(N_t^2M_t\right)$ and the matrix multiplication $\mathbf{F}_\mathrm{R}^{(k-1)^\dagger}\mathbf{F}_\mathrm{opt}$ to generate $\tilde{\mathbf{F}}_\mathrm{D}^{(k)}$ encompasses the complexity of $\mathcal{O}\left(N_tM_tN_s\right)$. Furthermore, the complexity in computing $\mathbf{M}^{(k)}$ is $\mathcal{O}\left(M_t^2N_s + N_tM_tN_s\right)$. The modified BCD, and the calculation of $\tilde{\mathbf{F}}_\mathrm{D}^{(k)}$ and $\mathbf{M}^{(k)}$ are repeated N_{it}^o times so that the complexity of MBCD-HP may be expressed as $N_{it}^o\mathcal{O}\big(N_{it}^i\left(N_t + M_t - 1\right)^2 + N_t^2M_t + 2N_tM_tN_s + M_t^2N_s\big)$. N_{it}^o and N_{it}^i represent the number of outer and inner iterations respectively.

The complexity of IPM-HP is largely determined by the computation of $\mathbf{M}\bar{\mathbf{F}}_\mathrm{R}^{(k-1)}$ and the adapted MGS orthogonalization performed on $\mathbf{M}\bar{\mathbf{F}}_\mathrm{R}^{(k-1)}$ using Algorithm 4 at each

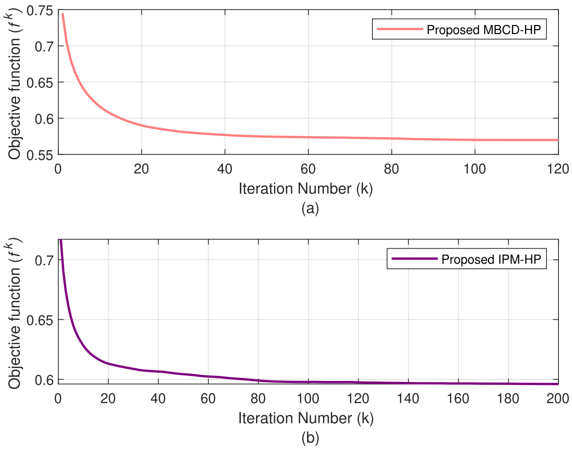

FIGURE 2. Convergence behavior of a) Proposed MBCD-HP a) Proposed IPM-HP in narrowband channel.

iteration k. The complexity involved in calculating $\mathbf{M}\bar{\mathbf{F}}_{\mathrm{R}}^{(k-1)}$ is $\mathcal{O}\left(N_t^2 M_t\right)$. The computational complexity of the adapted MGS orthogonalization in the Algorithm 4 is dictated by step 4-step 6. Even though the Algorithm 4 differs slightly from the actual MGS algorithm in step 8, we can still consider the computational complexity of the actual MGS algorithm which is $\mathcal{O}\left(N_t M_t^2\right)$ [31] (Chapter 5.2.8). Thus, the total complexity of computing analog precoder in the IPM-HP algorithm is $\mathcal{O}\left(N_{it} N_t^2 M_t + N_t M_t^2 + N_t^2 N_s\right)$ where N_{it} is the number of iterations performed and $\mathcal{O}\left(N_t^2 N_s\right)$ is the complexity associated with computing $\mathbf{M}$. Finally, determining $\mathbf{F}_{\mathrm{D}}$ brings about the complexity of $\mathcal{O}\left(N_t^2 M_t + N_t M_t N_s\right)$.

VII. SIMULATION RESULTS

We consider a point-to-point MIMO system with $N_t = 64$ antennas at the transmitter and $N_r = 16$ antennas at the receiver to assess the performance of the proposed precoding methods. We consider channel parameters $N_c = 5$, $N_p = 10$, $\alpha_{i\ell} \sim \mathcal{CN}(0, 1)$, as in [20]. The AoDs and AoAs are taken to be Laplacian distributed with their mean angles uniformly distributed over $[0, 2\pi]$ and angular spread of 10 degrees. The antenna elements are separated by a distance of half wavelength. We define the signal-to-noise ratio (SNR) used in the plots as SNR $= \frac{\rho}{\sigma_n^2}$. The number of data streams N_s is considered 4 in all figures except FIGURE 4 and FIGURE 8 where we consider spectral efficiency as N_s is varied. In all the figures, the number of RF chains at both the transmitter and receiver are considered equal to the number of data streams, *i.e.*, $M_t = M_r = N_s$. When SNR is not the varying parameter, it is taken as 0 dB. The fully digital precoding is taken as performance benchmark.

A. NARROWBAND CHANNEL

In FIGURE 2, we show the convergence behavior of the proposed MBCD-HP and IPM-HP algorithms averaged over 500 channel realizations. The objective function at the

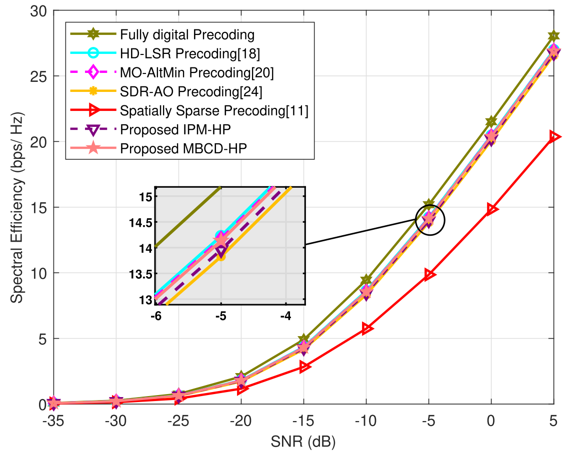

FIGURE 3. Spectral efficiency in narrowband channel as a function of SNR.

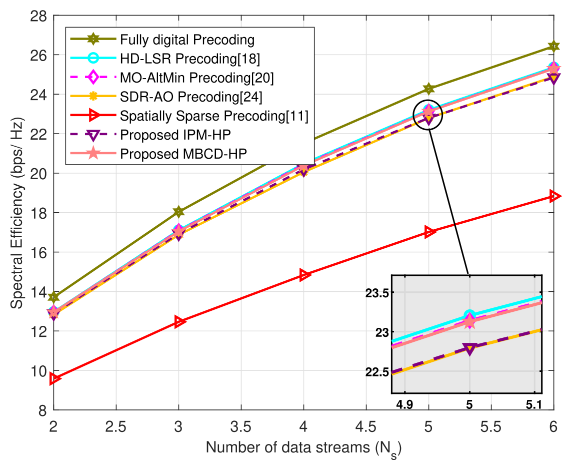

FIGURE 4. Spectral efficiency in narrowband channel as a function of number of data streams N_s.

iteration k, f^k is defined as $\left\|\mathbf{F}_{\mathrm{opt}} - \mathbf{F}_{\mathrm{R}}^{(k)}\mathbf{F}_{\mathrm{D}}^{(k)}\right\|_F^2$. It can be seen that both MBCD-HP and IPM-HP converge monotonically.

The spectral and bit error rate (BER) performances of the proposed algorithms are compared against SSP [11], the existing high-performing methods like HD-LSR [18], MO-AltMin [20] and SDR-AO [24]. The spectral efficiency is computed as $\log_2\left(\mathbf{I} + \frac{\rho}{\sigma_n^2 N_s}\mathbf{W}^{\dagger}\mathbf{H}\mathbf{F}\mathbf{F}^H\mathbf{H}^H\mathbf{W}\right)$.

In FIGURE 3 and FIGURE 4, the spectral performances of the proposed algorithms are examined with respect to other existing algorithms. The performance of MBCD-HP is very close to HD-LSR and MO-AltMin algorithms across all the values of SNR and N_s, and clearly better than SDR-AO. IPM-HP, while slightly behind MBCD-HP, also performs better than SDR-AO. The spectral performance of IPM-HP is very close to HD-LSR, MO-AltMin and MBCD-HP at lower values of N_s but diverges slightly away at higher N_s.

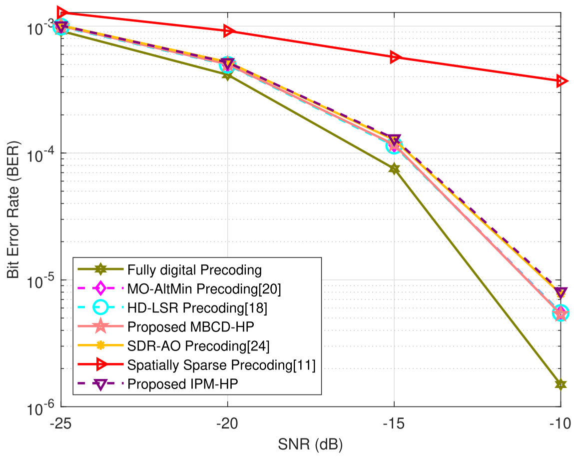

FIGURE 5. Bit Error Rate (BER) in narrowband channel as a function of SNR.

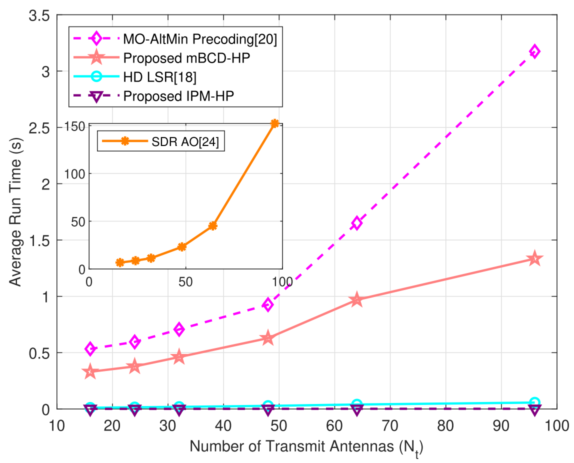

FIGURE 6. Average convergence times in narrowband channel for various precoding methods.

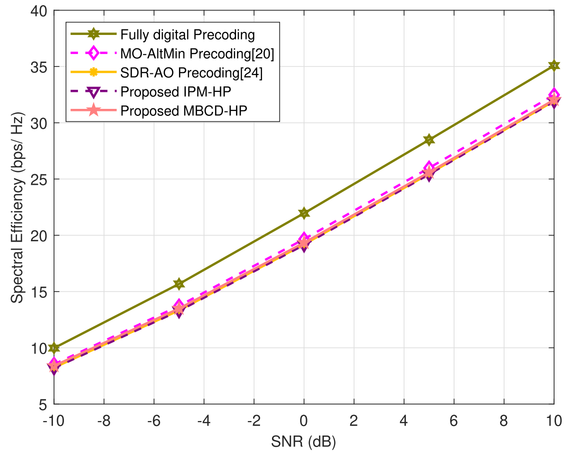

FIGURE 7. Spectral efficiency in wideband channel as a function of SNR.

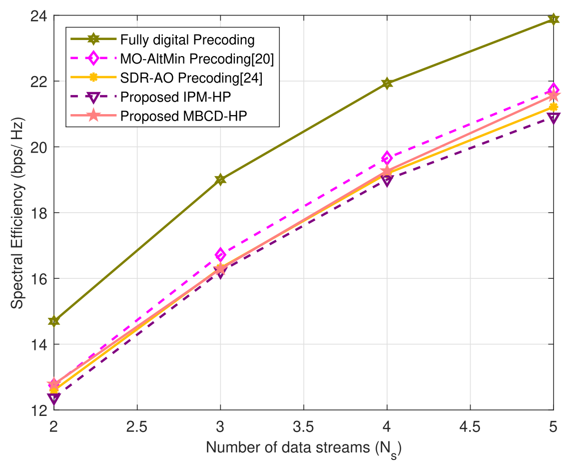

FIGURE 8. Spectral efficiency in wideband channel as a function of number of data streams N_s for $M_t = N_s$.

In FIGURE 5, we compare the BER performances of the proposed precoding methods with the existing hybrid precoders. The BER performance of MBCD-HP is similar to that of HD-LSR and they both exhibit the best performance among all other precoders. The performances of SDR-AO, MO-AltMin and IPM-HP are similar. However, the performance of SDR-AO gets better at higher SNR values. IPM-HP is slightly behind MO-AltMin and SDR-AO in BER performance, whereas SSP performs the poorest across all SNR values.

In FIGURE 6, we show how average run time of various algorithms vary versus the number of transmit antennas N_t. The plot for SDR-AO is produced in the inset to obtain an intelligible figure. All algorithms are run on 1.6 GHz Intel Core i5 PC with 8 GB RAM. It is evident that the convergence time of MBCD-HP is lower than that of MO-AltMin and very small compared to SDR-AO. For example at $N_t = 64$, the average run time are 45.08 seconds, 1.65 seconds, 0.9689 seconds, 0.0396 seconds, and 1.705 ms for SDR-AO, MO-AltMin, MBCD-HP, HD-LSR, and IPM-HP respectively. It is IPM-HP that proves to be the winner for having significantly lower convergence time compared to all the algorithms, including HD-LSR. HD-LSR comes with low complexity as well, however it is defined only for narrowband channel. The average run time increases with N_t for each of the algorithms. As far as average run time is concerned, SDR-AO is affected the most with the increase in N_t, followed by MO-AltMin. On the other hand, it is IPM-HP which is the least affected. As an instance, when N_t increases to 96, the average run time climbs to 152.3 seconds for SDR-AO, 3.175 seconds for MO-AltMin, 1.335 seconds for MBCD-HP, 0.05673 seconds for HD-LSR, and 1.88 ms for IPM-HP. It is apparent that the computational complexity and hence the run time rises steeply for SDR-AO and MO-AltMin as N_t increases.

B. WIDEBAND CHANNEL

The number of subcarriers S_c for the wideband channel is taken as 128. The spectral performance of the proposed algorithms is compared against the fully digital precoding, the existing high-performing methods like MO-AltMin [20] and SDR-AO [24]. Since HD-LSR and SSP are designed only for narrowband channel case, they are not considered for comparison in wideband channel.

We evaluate the spectral efficiency of the proposed algorithms in wideband channel as compared to the existing methods in FIGURE 7 and FIGURE 8. The performances of all the algorithms are close throughout the values of SNR with MO-AltMin performing the best, followed by MBCD-HP and SDR-AO. The performance of IPM-HP is behind all other methods. At lower values of N_s, MBCD-HP and SDR-AO are close in their performance, however MBCD-HP gets better at higher values of N_s. Similar to the case in narrowband channel, the spectral efficiency of IPM-HP deviates from those of other algorithms at higher values of N_s.

VIII. CONCLUSION

In this paper, we cast hybrid precoding in point-to-point mmWave MIMO narrowband channel as a trace optimization problem and propose two hybrid precoding algorithms. The first algorithm is an alternating minimization based algorithm MBCD-HP in which the analog precoding subproblem is cast as a semi-definite programming problem similar to PhaseCut after convex relaxation. The analog precoding problem is solved by the modified block coordinate descent method making use of the additional constraints compared to the usual PhaseCut. The hybrid precoding problem is separated into analog precoding subproblem and digital precoding subproblem in the second precoding method IPM-HP. The analog precoding subproblem is solved by an iterative algorithm similar to iterative power method used to determine the eigenvector matrix after enforcing orthogonality constraint on the analog precoder. The MBCD-HP algorithm produces very good spectral performance comparable to the state-of-art algorithms, and also comes with low complexity. The IPM-HP also produces good performance though slightly on the lower side compared to the MBCD-HP and the existing algorithms. However, IPM-HP comes with the benefit of extremely low complexity. Moreover, the proposed precoding methods can be extended to operate in wideband MIMO-OFDM channel. The good performance, coupled with low complexity and ability to operate on both narrowband and wideband channels make the proposed hybrid precoding algorithms promising.

REFERENCES

[1] Z. Pi and F. Khan, "An introduction to millimeter-wave mobile broadband systems," *IEEE Commun. Mag.*, vol. 49, no. 6, pp. 101–107, Jun. 2011.

[2] A. L. Swindlehurst, E. Ayanoglu, P. Heydari, and F. Capolino, "Millimeter-wave massive MIMO: The next wireless revolution?" *IEEE Commun. Mag.*, vol. 52, no. 9, pp. 56–62, Sep. 2014.

[3] F. Boccardi, R. W. Heath, Jr., A. Lozano, T. L. Marzetta, and P. Popovski, "Five disruptive technology directions for 5G," *IEEE Commun. Mag.*, vol. 52, no. 2, pp. 74–80, Feb. 2014.

[4] C.-X. Wang, F. Haider, X. Gao, X.-H. You, Y. Yang, D. Yuan, H. M. Aggoune, H. Haas, S. Fletcher, and E. Hepsaydir, "Cellular architecture and key technologies for 5G wireless communication networks," *IEEE Commun. Mag.*, vol. 52, no. 2, pp. 122–130, Feb. 2016.

[5] T. E. Bogale and L. B. Le, "Beamforming for multiuser massive MIMO systems: Digital versus hybrid analog-digital," in *Proc. IEEE Global Commun. Conf.*, Dec. 2014, pp. 4066–4071.

[6] R. W. Heath, Jr., N. González-Prelcic, S. Rangan, W. Roh, and A. M. Sayeed, "An overview of signal processing techniques for millimeter wave MIMO systems," *IEEE J. Sel. Topics Signal Process.*, vol. 10, no. 3, pp. 436–453, Apr. 2016.

[7] S. Han, C. I. Z. Xu, and C. Rowell, "Large-scale antenna systems with hybrid analog and digital beamforming for millimeter wave 5G," *IEEE Commun. Mag.*, vol. 53, pp. 186–194, Jan. 2015.

[8] A. Alkhateeb, J. Mo, N. Gonzalez-Prelcic, and R. W. Heath, Jr., "MIMO precoding and combining solutions for millimeter-wave systems," *IEEE Commun. Mag.*, vol. 52, no. 12, pp. 122–131, Dec. 2014.

[9] X. Gao, L. Dai, Y. Sun, S. Han, and I. Chih-Lin, "Machine learning inspired energy-efficient hybrid precoding for mmWave massive MIMO systems," in *Proc. IEEE Int. Conf. Commun. (ICC)*, May 2017, pp. 1–6.

[10] J.-C. Chen, "Constructive interference-based symbol-level precoding design for millimeter-wave massive multiuser MIMO systems with hardware-efficient hybrid precoding architecture," *IEEE Access*, vol. 9, pp. 18393–18401, 2021.

[11] O. El Ayach, S. Rajagopal, S. Abu-Surra, Z. Pi, and R. W. Heath, Jr., "Spatially sparse precoding in millimeter wave MIMO systems," *IEEE Trans. Wireless Commun.*, vol. 13, no. 3, pp. 1499–1513, Jan. 2014.

[12] D. H. Nguyen, L. B. Le, T. Le-Ngoc, and R. W. Heath, Jr., "Hybrid MMSE precoding and combining designs for mmWave multiuser systems," *IEEE Access*, vol. 5, pp. 19167–19181, 2017.

[13] M. Kim and Y. H. Lee, "MSE-based hybrid RF/baseband processing for millimeter-wave communication systems in MIMO interference channels," *IEEE Trans. Veh. Technol.*, vol. 64, no. 6, pp. 2714–2720, Jun. 2015.

[14] A. Alkhateeb, G. Leus, and R. W. Heath, Jr., "Limited feedback hybrid precoding for multi-user millimeter wave systems," *IEEE Trans. Wireless Commun.*, vol. 14, no. 11, pp. 6481–6494, Nov. 2015.

[15] W. Ni and X. Dong, "Hybrid block diagonalization for massive multiuser MIMO systems," *IEEE Trans. Commun.*, vol. 64, no. 1, pp. 201–211, Jan. 2016.

[16] P. R. Gautam and L. Zhang, "Hybrid SLNR precoding for multi-user millimeter wave MIMO systems," in *Proc. 22nd Int. Symp. Wireless Pers. Multimedia Commun. (WPMC)*, Nov. 2019, pp. 1–6.

[17] F. Sohrabi and W. Yu, "Hybrid digital and analog beamforming design for large-scale antenna arrays," *IEEE J. Sel. Topics Signal Process.*, vol. 10, no. 3, pp. 501–513, Apr. 2016.

[18] C. Rusu, R. Mèndez-Rial, N. González-Prelcic, and R. W. Heath, Jr., "Low complexity hybrid precoding strategies for millimeter wave communication systems," *IEEE Trans. Wireless Commun.*, vol. 15, no. 12, pp. 8380–8393, Dec. 2016.

[19] S. Payami, M. Ghoraishi, and M. Dianati, "Hybrid beamforming for large antenna arrays with phase shifter selection," *IEEE Trans. Wireless Commun.*, vol. 15, no. 11, pp. 7258–7271, Nov. 2016.

[20] X. Yu, J.-C. Shen, J. Zhang, and K. B. Letaief, "Alternating minimization algorithms for hybrid precoding in millimeter wave MIMO systems," *IEEE J. Sel. Topics Signal Process.*, vol. 10, no. 3, pp. 485–500, Apr. 2016.

[21] T. Lin, J. Cong, Y. Zhu, J. Zhang, and K. Ben Letaief, "Hybrid beamforming for millimeter wave systems using the MMSE criterion," *IEEE Trans. Commun.*, vol. 67, no. 5, pp. 3693–3708, May 2019.

[22] J. Cong, T. Lin, and Y. Zhu, "Hybrid MMSE beamforming for multiuser millimeter-wave communication systems," *IEEE Commun. Lett.*, vol. 22, no. 11, pp. 2390–2393, Nov. 2018.

[23] A. Arora, C. G. Tsinos, B. S. M. R. Rao, S. Chatzinotas, and B. Ottersten, "Hybrid transceivers design for large-scale antenna arrays using majorization-minimization algorithms," *IEEE Trans. Signal Process.*, vol. 68, pp. 701–714, 2020.

[24] X. Qiao, Y. Zhang, M. Zhou, and L. Yang, "Alternating optimization based hybrid precoding strategies for millimeter wave MIMO systems," *IEEE Access*, vol. 8, pp. 113078–113089, 2020.

[25] S. Boyd and L. Vandenberghe, *Convex Optimization*. Cambridge, U.K.: Cambridge Univ. Press, 2004.

[26] I. Waldspurger, A. D'Aspremont, and S. Mallat, "Phase recovery, MaxCut and complex semidefinite programming," *Math. Programm.*, vol. 149, nos. 1–2, pp. 47–81, 2015.

[27] Z. Wen, D. Goldfarb, and K. Scheinberg, *Block Coordinate Descent Methods for Semidefinite Programming*. Boston, MA, USA: Springer, 2012, pp. 533–564.

[28] H. Rutishauser, "Computational aspects of F. L. Bauer's simultaneous iteration method," *Numerische Math.*, vol. 13, no. 1, pp. 4–13, Mar. 1969.

[29] A. Björck, "Numerics of Gram-Schmidt orthogonalization," *Linear Algebra Appl.* vols. 197–198, pp. 297–316, Jan./Feb. 1994.

[30] J. Lee and Y. H. Lee, "AF relaying for millimeter wave communication systems with hybrid RF/baseband MIMO processing," in *Proc. IEEE Int. Conf. Commun. (ICC)*, Jun. 2014, pp. 5838–5842.

[31] G. H. Golub and C. F. Van Loan, *Matrix Computations*, 4th ed. Baltimore, MD, USA: Johns Hopkins Univ. Press, 2013.

PRABHAT RAJ GAUTAM (Graduate Student Member, IEEE) received the Bachelor of Engineering degree in electronics and communications engineering from the Institute of Engineering, Tribhuvan University, Nepal, in 2010, and the Master of Technology degree in communications engineering from the Indian Institute of Technology (IIT) Delhi, New Delhi, India, in 2015. He is currently pursuing the Ph.D. degree with the School of Electronic and Electrical Engineering, University of Leeds, Leeds, U.K. His current research interests include millimeter wave communications and signal processing for communications and hybrid precoding for millimeter wave communications. He received the Best Student Paper Award at the International Symposium on Wireless Personal Multimedia Communications (WPMC), in 2019.

LI ZHANG (Senior Member, IEEE) received the Ph.D. degree in communications from the University of York, in 2003. Currently, she is an Associate Professor and leads the Wireless Communication Group, School of Electronic and Electrical Engineering, University of Leeds, U.K. Her research interests include wireless communications and signal processing techniques, such as massive MIMO, mmWave communications, heterogeneous networks, device to device communications, and 5G systems. She has been serves on the technical program committees of most major IEEE conferences in communications, since 2006, and is an associate editor of IEEE journals. She has been selected as a member of the prestigious U.K. EPSRC Peer Review College, since 2006, and regularly helps reviewing grant applications for research councils and book proposals. She has been a Ph.D. examiner for numerous universities. In 2005, she received a Nuffield Award for a newly appointed lecturer. In 2006, she became a fellow of Higher Education Academy. In 2011, she was awarded as an IEEE Exemplary Reviewer.